Matt Thacker
GE 712 and 805
Final Project
4-28/18

Relating Spatial Heterogeneity in Extreme Temperatures to Sulfate Aerosols using Spatial Simultaneous Autoregressive Error Models

Introduction:

Atmospheric sulfate aerosols have long been known to have a cooling effect on global climate. By reflecting and scattering incoming radiation in the atmosphere before it reaches the surface of the earth sulfate aerosols contribute negatively to global radiative forcing (Haywood and Boucher, 2000). Radiative forcing in turn, has been shown to be strongly positively related to patterns in global temperature change (Estrada *et al.*, 2013). Additionally, aerosols have been shown to have an indirect cooling effect on global climate by providing clouds with additional condensation nuclei, increasing the scattering and thermal absorption properties of clouds by increasing the drop concentrations within them (Boucher *et al.*, 2013; Gettleman *et al.*, 2015).

Many studies examining the relationship between radiative forcing and temperature have focused on comparing radiative forcing to aggregate measures of temperature such as monthly or annual means. While this approach offers significant insight into the overall warming trend in the temperature record following the Industrial Revolution, it does not adequately address the increases in extreme temperatures which have been observed over that same time period (Alexander, 2016). In order to address this, many recent studies have directly compared measures of radiative forcing, particularly forcing due to human activities, to extreme temperature events on a wide variety of spatial scales, and have demonstrated strong relationships between them (Wen *et al.*, 2013).

Additionally, extreme temperature events have been related to the general public's understanding of climate science by Kaufmann *et al.* (2017). Because the effects of climate change are not evenly distributed over space, it is logical to assume that individual experiences with those effects are likewise unevenly distributed. Kaufmann *et al.* (2017) demonstrated a link between this spatial heterogeneity and public skepticism of climate science by showing a relationship between an index of local extreme temperatures known as *Tmax* and county based estimates of percent belief in global warming generated by Howe *et al.* (2015). Areas with higher frequencies of extreme high temperatures were more likely to believe in climate science and vice versa (Kaufmann *et al.*, 2017).

The apparent importance of extreme temperature events in determining the public perception of the state of the climate and its inter-annual changes implies a need to better understand the specific drivers of the spatial heterogeneity in extreme temperatures. Previous studies have demonstrated the negative radiative forcing of sulfate aerosols and the connection between local radiative forcing totals and extreme temperatures, but there has not been research which explicitly links the effects of sulfate aerosols to extreme temperature events.

This project examines that relationship using the indexes of local extreme temperatures sourced from Kaufmann *et al.* (2017) and spatial data relating to the radiative forcing effects of sulfur aerosols. Spatial simultaneous error models which account for spatial autocorrelation in the error term are estimated between long term and recent measurements of high and low temperature frequency and the top of atmosphere energy balance differences associated with sulfate aerosols.

Data and Methods:

Vector polyline data containing measures of local extreme temperatures as described in Kaufmann et al. (2010) associated with census blocks in the continental U.S. were obtained from Professor Michael Mann. Four indices based on the temperature record of a given weather station, *Tmax, Tmin*, *High2005*, and *Low2005* were used in this study. *Tmax* is calculated by comparing the date of the record high and low temperature for each day of the year at a given weather station. The index is simply number of dates for which the record high is greater than the record low and can be specified thusly:

$$Tmax_i = \sum_{D=1}^{365} (High_{D_i} > Low_{D_i}) x1$$

Tmin is a nearly identical calculation except that it represents the number of days for which the record low is more recent than the record high:

$$Tmin_i = \sum_{D=1}^{365} (High_{D_i} < Low_{D_i}) x1$$

High2005 and *Low2005* were used to introduce recency weighting to the regressions estimated in Kuafmann *et al*. (2017) and can be imagined as analogues of *Tmax* and *Tmin* which only draw from high or low temperatures observed after 2005:

$$High2005_i = \sum_{D=1}^{365} [(High_{D_i} > Low_{D_i}) x1 x (High_{D_i} => 2005)]$$

$$Low2005_i = \sum_{D=1}^{365} [(High_{D_i} < Low_{D_i}) x1 x (Low_{D_i} => 2005)]$$

As a part of the analysis performed in Kaufmann *et al.* (2017) these indices for each station were associated with all census blocks which were closer to that station than any other using Thiessen polygons.

Additionally, a global raster data set representing the top of atmosphere (TOA) energy balance differences due to radiative forcing by sulfur aerosols averaged from 2001-2010 was obtained from Professor Michael Mann. The data are recorded at relatively coarse spatial resolution (approximately 300km pixel size), and their values can be interpreted as the magnitude of radiative forcing applied by sulfur aerosols. Smaller and particularly negative values indicate a cooling affect.

Prior to statistical analysis, geoprocessing steps were performed using ArcGIS to allow for easy computation of the statistical models. First, the global TOA flux raster was clipped to the spatial extent of the census tracts shapefile. This was done to remove unnecessary data from the analysis and to speed up future geoprocessing steps. Additionally, each census tract was assigned an associated flux value using spatial joins. For each census tract, a new attribute was added which corresponded to the value in the flux raster cell in which its centroid was located. Because each raster cell was far larger than each census tract, the join one to many option was used to ensure that each cell was permitted to be joined to more than one census tract. Finally, in order to facilitate processing on my older personal computer, the data were converted into point data representing the centroid of each tract rather than a polygon representing the tract itself. This did not interfere with the analysis as the spatial weights matrices used in the analysis would be based on centroid points anyway as that is the default implementation in R which was used for the statistical analysis.

Preliminary models were estimated using simple ordinary least squares (OLS) regression techniques between *Tmax, Tmin*, *High2005*, *Low2005* and TOA flux. Each model took the same basic form which can be described as:

$$Index_i = B_0 + B_1 Flux + \epsilon$$

Where ε is a normally distributed uncorrelated error term with mean 0. All models were fit using R.

Because of the large scale patterns of temperature and climate more generally in the U.S., spatial autocorrelation is highly likely in the variables considered in these models. If such autocorrelation exists, these models are likely to violate the OLS assumption of an uncorrelated error term as the spatial pattern in the data would be unaccounted for in the model and thus passed into the error term. Following the methodology described in Kaufmann *et al.* (2017) the Moran's I test for spatial autocorrelation was applied to the residuals of each preliminary model using the lm.morantest() function from R's spdep package. Moran's I tests the degree to which each observation covaries with its neighbors weighted by the distance that neighbor is to the observation at hand. It can be written as:

$$I = \frac{N}{W} \frac{\sum_i \sum_j w_{ij}(x_i - \bar{x})(x_j - \bar{x})}{\sum_i (x_i - \bar{x})^2}$$

Where N is the sum of available spatial units, W is the sum of all available spatial weights, w_{ij} is the spatial weight between locations i and j, and x_i, x_j, and $\bar{x}$ are the values associated with locations i and j and the mean value respectively.

Because spatial autocorrelation was detected in the residuals from all models, it was necessary to include a spatial lag or error term in the models. Again, following the method of Kaufmann *et al.*, (2017) robust versions of the Lagrange multiplier test for spatially dependent linear models were performed using the lm.LMtests() function in the spdep package. The robust Lagrange multiplier test for spatially dependent models considers a model of the general form:

$$y = \rho W_1 y + XB + \epsilon$$

$$\epsilon = \lambda W_2 \epsilon + \mu$$

Where B is the vector of coefficients corresponding to the covariates X, ρ is the coefficient corresponding to the spatially lagged dependent variable y, W_1 and W_2 are the spatial weights matrices associated with the autoregressive process in the lagged variable and error term respectively, λ is the coefficient corresponding to the spatial error term ϵ, and μ is a well behaved error term. By testing the null hypotheses that ρ or λ are equal to 0 the test can detect the presence of a missing spatial lag or error term in the models considered. The robust version of the test allows for a non-0 number of nuisance parameters in the specification of either model to account for the possibility of the presence of both processes in the data. The exact derivation of this test is complex and beyond the scope of this paper, but more information can be found in Anselin (2010).

Lagrange multiplier tests indicated that spatial error models were appropriate for all models under consideration. Spatial simultaneous autoregressive error models were estimated between each index and TOA flux using maximum likelihood estimation as implemented in the errorsarlm() function in the spdep package. Spatial error models are a special case of the general form used in the Lagrange multiplier test described above, and can be written as:

$$y = \alpha + XB + \epsilon$$

$$\epsilon = \lambda W \epsilon + \mu$$

Only the values α and B coefficients are of interest in this analysis, the parameters estimated in ϵ are best thought of as nuisance parameters.

Results:

Table 1 shows the results of the Moran's I and Lagrange Multiplier tests for the models estimated with each index as the dependent variable. These results show the clear presence of spatial autocorrelation in the OLS residuals ($p<.001$) for all models. Additionally although both the spatial lag and error terms are significant for many of the models as per the Lagrange multiplier test, in each case the results are more significant for the error term which supports the use of spatial error rather than spatial lag models.

Table 2 displays the estimated coefficients and associated p values for each simultaneous autoregressive error model. The most important thing to note here is that although all models estimate highly significant coefficients, the signs on those coefficients do not completely conform to how one would expect given the relationships between dependent variables. Specifically, while the coefficients associated with *Tmax* and *Tmin* are the opposite of one another in terms of sign the coefficients on *High2005* and *Low2005* are both positive. As high values of *Tmax* or *High2005* generally indicate a warming trend, the opposite of the cooling trend indicated by *Tmin* and *Low2005* the two groups would be expected to produce oppositely signed coefficients.

The most probable explanation for these incongruous results lies in the limited samples available for *Low2005*. Due to the low frequency of extreme low temperatures in recent years, the variation present in *Low2005* did not capture the process this study was interested in. In other words, in general across the continental United States there have not been a large or varied enough number of record low days since 2005 for any clear effect of sulfate aerosols to be visible. Figure 1 shows a histogram of *Low2005* and Table 3 compares the variances in each

index used in this study. From them we can clearly see that *Low2005* is highly inflated by 0's and other low values and its variance is diminished compared to both *High2005* and *Tmax* and *Tmin*. This diminished variance meant that the models estimated using *Low2005* are based on a much weaker signal than the other models, particularly those estimated using *Tmax* and *Tmin* for the entire time period.

Discussion:

The diminished variance of *Low2005* and to a lesser extent *High2005* implies that the data underlying these metrics may not contain enough information relevant for this analysis. Accordingly, the remainder of this paper will focus solely on the models estimated using *Tmax* and *Tmin* across the full time period.

Because smaller TOA flux values indicate a cooling affect due to sulfur, one would expect TOA flux to be positively associated with the frequency of extreme high temperatures (*Tmax*) and negatively with the frequency of extreme low temperatures (*Tmin).* Regression results which account for the presence of spatial non-stationarity in the data show a relationship between radiative forcing due to sulfur aerosols and the frequency of local maximum or minimum temperatures. The signs on the coefficients estimated, positive for *Tmax* and negative for *Tmin*, conform to our understanding of the climate system and the role of sulfate aerosols therein.

There are however many sources of potential errors or inconsistency which must be discussed. The coarse spatial resolution (300km pixels) of the TOA flux raster which provided the independent variable for all models estimated is one such source. Because the measures of

Tmax and *Tmin* were originally sourced from weather stations distributed on a much finer spatial scale than the flux data, there are many values of *Tmax* and *Tmin* associated with each distinct flux value (Kaufmann *et al.*, 2017). This results in a large degree of noise in the relationships considered in these models, as the resolution of the flux data is far too large to capture many patterns present in the indices.

An additional source of error is the temporal inconsistencies which permeate the data used in this analysis. Each weather station used in the *Tmax* and *Tmin* calculations represents a unique and non-standardized reporting period and thus the values in those indices are not calculated for a consistent time frame (Kaufmann *et al.*, 2017). Additionally, the reporting period for those stations stretches back decades but the TOA flux raster only provides data from 2001-2010. These temporal inconsistencies may cause erroneous results because the processes which drove the observed data may not be accounted for in the observed covariates, thus introducing an omitted variable bias.

While these results suggest that there may be discernable relationship between radiative forcing due to sulfate aerosols and measures of local extreme temperature events, more analysis is necessary to determine their robustness. Performing similar analyses using flux data of a smaller spatial scale and more temporally aligned measures of *Tmax* and *Tmin* could provide significant insight into whether the results observed in this study are an artifact of the data used or reflective of geographic reality. Such tests are necessary due to the aforementioned issues with the data used in this project, as well as the incongruent results between the models estimated for the whole time period and those from 2005 on. If these results are robust, they point to a specific,

if somewhat expected cause of the spatial heterogeneity in the effects of climate change observed in Kaufmann *et al.* (2017).

References:

Alexander, Lisa V. "Global Observed Long-Term Changes in Temperature and Precipitation Extremes: A Review of Progress and Limitations in IPCC Assessments and Beyond." *Weather and Climate Extremes*, vol. 11, 2016, pp. 4–16., doi:10.1016/j.wace.2015.10.007.

Anselin, Luc. "Lagrange Multiplier Test Diagnostics for Spatial Dependence and Spatial Heterogeneity." *Geographical Analysis*, vol. 20, no. 1, 2010, pp. 1–17., doi:10.1111/j.1538-4632.1988.tb00159.x.

Boucher, O., D. Randall, P. Artaxo, C. Bretherton, G. Feingold, P. Forster, V.-M. Kerminen, Y. Kondo, H. Liao, U. Lohmann, P. Rasch, S.K. Satheesh, S. Sherwood, B. Stevens, and X.Y. Zhang, 2013: Clouds and aerosols. In Climate Change 2013: The Physical Science Basis. Contribution of Working Group I to the Fifth Assessment Report of the Intergovernmental Panel on Climate Change. T.F. Stocker, D. Qin, G.-K. Plattner, M. Tignor, S.K. Allen, J. Doschung, A. Nauels, Y. Xia, V. Bex, and P.M. Midgley, Eds. Cambridge University Press, pp. 571-657, doi:10.1017/CBO9781107415324.016.

Estrada, Francisco, et al. "Statistically Derived Contributions of Diverse Human Influences to Twentieth-Century Temperature Changes." *Nature Geoscience*, vol. 6, no. 12, 2013, pp. 1050–1055., doi:10.1038/ngeo1999.

Gettelman, A., et al. "Impact of Aerosol Radiative Effects on 2000â2010 Surface Temperatures." *Climate Dynamics*, vol. 45, no. 7-8, 2015, pp. 2165–2179., doi:10.1007/s00382-014-2464-2.

Haywood, James, and Olivier Boucher. "Estimates of the Direct and Indirect Radiative Forcing Due to Tropospheric Aerosols: A Review." *Reviews of Geophysics*, vol. 38, no. 4, 2000, pp. 513–543., doi:10.1029/1999rg000078.

Howe, Peter D., et al. "Geographic Variation in Opinions on Climate Change at State and Local Scales in the USA." *Nature Climate Change*, vol. 5, no. 6, 2015, pp. 596–603., doi:10.1038/nclimate2583.

Kaufmann, Robert K., et al. "Spatial Heterogeneity of Climate Change as an Experiential Basis for Skepticism." *Proceedings of the National Academy of Sciences*, vol. 114, no. 1, 2016, pp. 67–71., doi:10.1073/pnas.1607032113.

Wen, Qiuzi Han, et al. "Detecting Human Influence on Extreme Temperatures in China." *Geophysical Research Letters*, vol. 40, no. 6, 2013, pp. 1171–1176., doi:10.1002/grl.50285.

Figures and Tables:

Table 1. Spatial diagnostic statistics for all models

Dependent Variable	Moran's I Statistic Standard Deviate	Lagrange Multiplier Statistic for Spatial Lag	Lagrange Multiplier Statistic for Spatial Error
Tmax	465.11 ($p < 2*10^{-16}$)	17.166 ($p = 3.424*10^{-5}$)	66.593 ($p = 3.331*10^{-16}$)
Tmin	455.22 ($p < 2*10^{-16}$)	52.098 ($p = 5.279*10^{-13}$)	148.29 ($p < 2*10^{-16}$)
High2005	432.91 ($p < 2*10^{-16}$)	.27809 ($p = .598$)	21.784 ($p = 3.052*10^{-6}$)
Low2005	426.1 ($p < 2*10^{-16}$)	.75861 ($p = .3838$)	11.929 ($p = 5.526*10^{-4}$)

Table 2. Spatial regression results for all models

Dependent Variable	α	*B*	λ
Tmax	223.179 ($p < 2*10^{-16}$)	6.248 ($p < 2*10^{-16}$)	.94 ($p < 2*10^{-16}$)
Tmin	132.158 ($p < 2*10^{-16}$)	-9.676 ($p < 2*10^{-16}$)	.932 ($p < 2*10^{-16}$)
High2005	56.421 ($p < 2*10^{-16}$)	2.982 ($p = 2.11*10^{-15}$)	.912 ($p < 2*10^{-16}$)
Low2005	22.734 ($p < 2*10^{-16}$)	1.845 ($p = 1.672*10^{-12}$)	.909 ($p < 2*10^{-16}$)

Table 3. Variance of each index used as a dependent variable

Index	Variance
Tmax	1834.354
Tmin	1584.303
High2005	514.296
Low2005	244.89

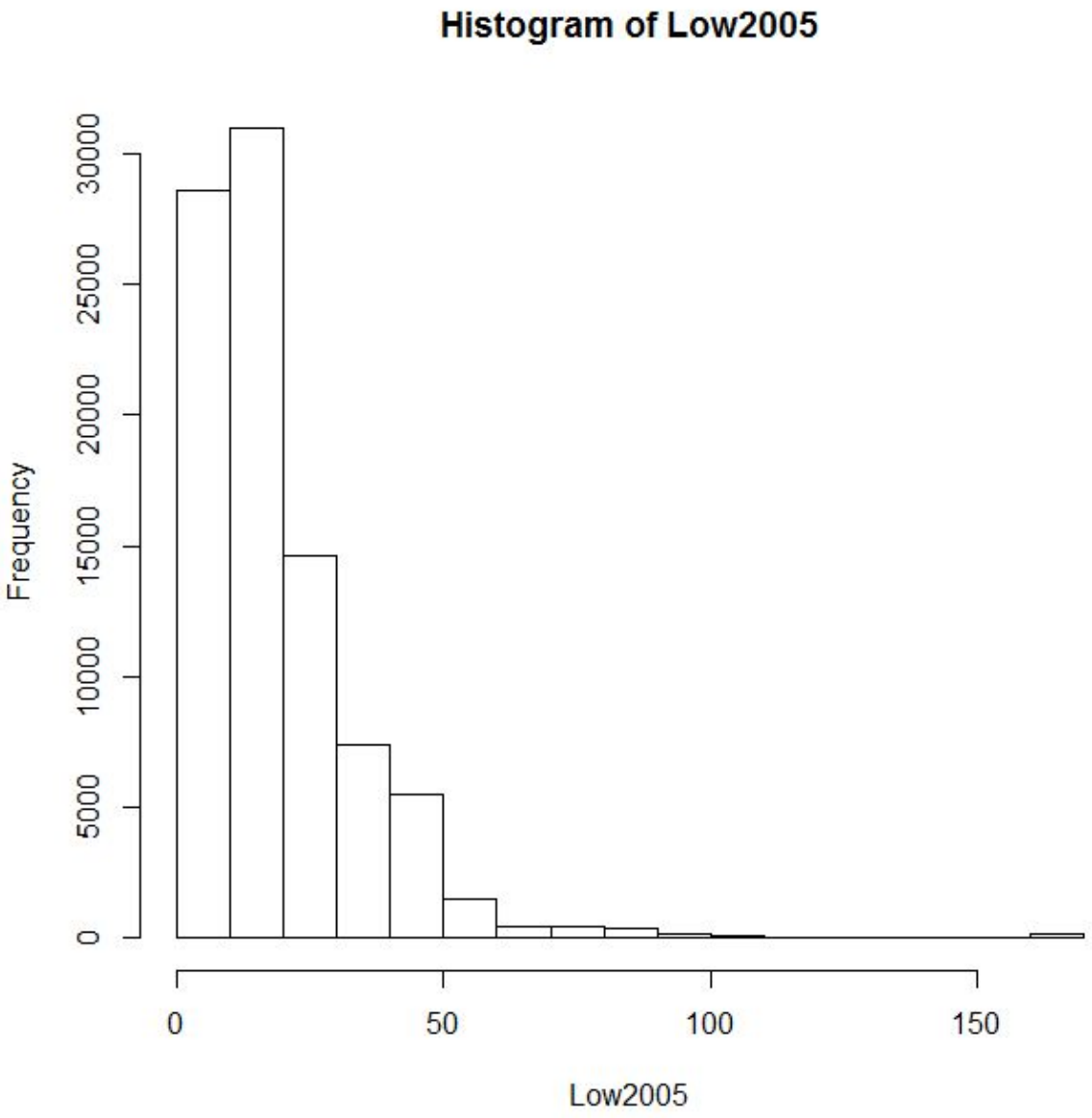

Figure 1. Histogram of the *Low2005* index as used in this paper